

Computer Numerical Control Machining Simulations and Experimental Analysis of a Novel C-Gear

Qi ZHANG*,**,***, Zhixin CHEN****, Yongjie XIA****, Dongcheng HE*****,
Guoqi XIANG*****, Guang WEN*****, Xuegang ZHANG*****,
Yongchun XIE*****, Guangchun YANG*****

*Chengdu Technological University, Chengdu, 611730, China, E-mail: pzhuzq@126.com (Corresponding author)

**Chengdu Industrial Vocational Technical College, Chengdu, 610218, China

***Panzhuhua university, Panzhuhua, 617000, China

****Chengdu Industry and Trade College, 601165, Chengdu, China

*****Sichuan University of Science & Engineering, Yibin, 644000, China, E-mail: m18208107365@163.com

*****Panzhuhua university, Panzhuhua, 617000, China, E-mail: 1149363255@qq.com

*****Panzhuhua university, Panzhuhua, 617000, China, E-mail: 191870261@qq.com

*****Chengdu Industrial Vocational Technical College, Chengdu, 610218, China, E-mail: 57438701@qq.com

*****Panzhuhua university, Panzhuhua, 617000, China, E-mail: 583930414@qq.com

*****Panzhuhua university, Panzhuhua, 617000, China, E-mail: 493694786@qq.com

*****Panzhuhua university, Panzhuhua, 617000, China, E-mail: 1297208354@qq.com

<https://doi.org/10.5755/j02.mech.35514>

1. Introduction

The concept of C-gear, a type of parallel shaft transmission gear with circular arc teeth, was first proposed by the German scholar Bottcher in 1913 [1]. Since its ideation, several studies have investigated the machining methods for the C-gear. Ishibashi et al. [2] and Inoue et al. [3] proposed gear grinding and burnishing methods to improve the machining accuracy of C-gear. Koga et al. proposed a hypoid format tilt that can cut the concave and convex tooth surfaces of the gear teeth simultaneously for machining the C-gear [4]. Peng et al. used a circular broach to machine the C-gear, which satisfied the single-tooth division requirement for machining gears with the hypoid format tilt and improved the gear processing efficiency [5]. Tseng et al. [6] used rotary cutter heads with a double-sided milling tool to construct the C-gear. Andrei et al. established the mathematical model for the concave and convex tooth surfaces of the C-gear by employing the single-edge method using a rotary cutter head, and performed the cutting tests [7]. MA et al. [8, 9] used double-blade rotary cutters with a knife angle to construct a C-gear, and realized the computer numerical control (CNC) machining of the completely modified tooth surface of the gear. Tseng et al. [10, 11] and Dai et al. [12] successively proposed and studied the hobbing machining method for the C-gear, and realized continuous cutting of the gear teeth. Song et al. [13] used parallel linkage for milling and obtained a C-gear with an involute tooth profile in all the cross sections. Uzun et al. [14] used a wire electrical discharge machining (EDM) manufactured involute mouth-profile end mill cutter to realize the CNC milling of a C-gear. Zhang et al. [15] constructed a 6-axis CNC tool model to simulate the C-gear machining process on the VERICUT software based on its generation principle.

Based on the abovementioned studies, the circular arc tooth line cylindrical gear machining methods can be summarized into the following four categories: 1. rotary cutter milling, 2. gear hob hobbing, 3. translative device milling, 4. cutter milling with cutter angle. Among these, the most commonly employed is the rotary cutter milling

method. Its processing principle is consistent with the C-gear generation principle, but it requires a special processing machine, different processing modules, different tool radii, and various types of profile structures. Due to the increased complexity of the cutter and machining tools, this method is not suitable for the development of a new type of C-gear, in terms of both cost and preparation time.

In this study, a 5-axis CNC tool is used to construct a C-gear with an improved structure, while solving the prototype manufacturing problem. The C-gear mathematical model was deduced and the three-dimensional (3D) modeling method with high precision based on its development principle was studied. The C-gear processing technique using the 5-axis CNC machining center was established, the tool path was designed, and the process was simulated using the MASTERCAM and VERICUT software. The machining method studied in this paper is less efficient than the rotary cutter milling method, but vastly economical and less time consuming. It provides an effective way to construct an improved C-gear for practical application.

2. C-gear generation principle

The tooth line of the C-gear analysed in this study is a spatial circular arc (Fig. 1). The middle section tooth profile is an involute and the other cross sections are uniformly changing hyperbolic enveloping lines [5, 6]. The circular arc tooth line cylindrical gear has the following advantages:

1. which is not sensitive to the installation coaxiality error, and exhibits low noise and stable performance compared to the straight-toothed gears;
2. there is no axial force, and does not cause additional load on the bearing compared to the helical gears;
3. which has a higher contact ratio compared to the herringbone toothed gears, but a better processing efficiency and a simpler assembly process due to the absence of the tool withdrawal groove.

In order to establish the tooth surface equation of

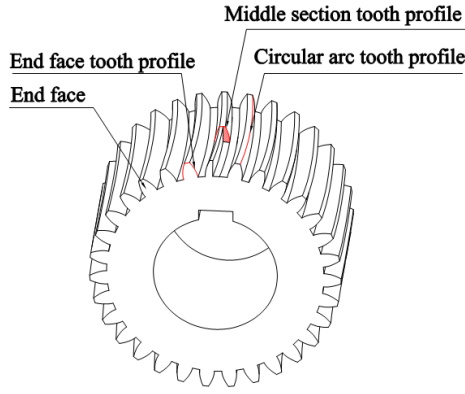


Fig. 1 Schematic representation of the examined C-gear

the C-gear, firstly setup the coordinate system (Fig. 2) according to its generation principle: $O_t - x_t, y_t, z_t$ is the fixed coordinate system of the rotary cutter head; $O_g - x_g, y_g, z_g$ and $O_d - x_d, y_d, z_d$ are the moving and dynamic coordinate systems of the gear blank, respectively; R_g is the pitch circle radius of the gear blank, ψ is the gear blank rotation angle, R_t is the nominal radius of the cutter head, θ is the rotation angle of the cutter head, and B is the tooth width.

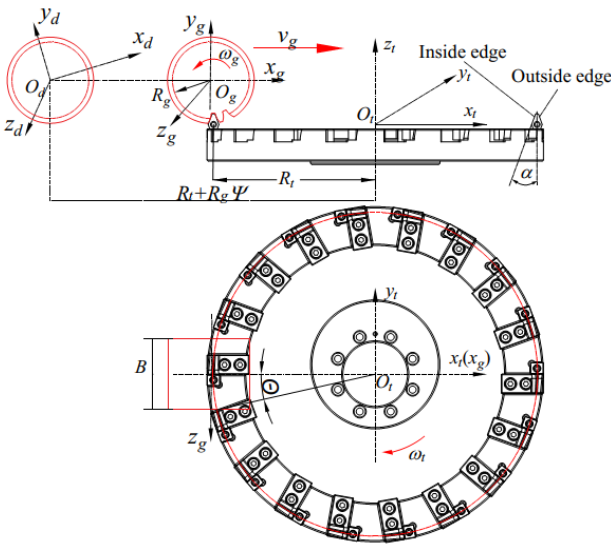


Fig. 2 C-gear coordinate system based on its generation principle

The rotary cutter head for processing the C-gear is installed on the spindle of the machine tool, which rotates around z_t . The double-edge milling cutter fixed on the rotary cutter head rotates with it simultaneously. It can cut two conical faces on the workpiece after one rotation: the outer cutting edge cuts a positive cone (to realize the concave machining of the gear) and the inner cutting edge cuts a negative cone (to realize the convex machining of the gear). During the milling process, the workpiece rotates around the z_g axis while moving in the horizontal direction, inducing a gear generation movement between itself and the double-edge milling cutter. The milling tool simultaneously processes both concave and convex tooth surfaces. After processing a tooth, the next tooth is divided and the process continues until the complete gear is constructed.

3. C-gear tooth surface equation

3.1. Double-edge milling cutter revolution surface equation

In the $O_t - x_t, y_t, z_t$ coordinates, the double-edge milling cutter revolution surface equation can be defined as [16–19]:

$$\begin{cases} x_t = -\left(R_t \mp \frac{\pi}{4} m \pm u \sin \alpha\right) \cos \theta \\ y_t = -\left(R_t \mp \frac{\pi}{4} m \pm u \sin \alpha\right) \sin \theta, \\ z_t = u \cos \alpha \end{cases} \quad (1)$$

where \mp and \pm represent the inner and outer cutting edges, respectively, α is the cutter angle, m is the modulus, and u is the distance between a point on the cutter surface and the pitch point along the generatrix direction. In the $O_t - x_t, y_t, z_t$ coordinates, the double-edge milling cutter revolution surface equation can be rewritten as:

$$\begin{aligned} \mathbf{r}_t = & -\left(R_t \mp \frac{\pi}{4} m \pm u \sin \alpha\right) \cos \theta \mathbf{i} + u \cos \alpha \mathbf{k} - \\ & -\left(R_t \mp \frac{\pi}{4} m \pm u \sin \alpha\right) \sin \theta \mathbf{j}, \end{aligned} \quad (2)$$

with a unit normal vector defined as [16-19]:

$$\begin{aligned} \mathbf{n}_t = \frac{\partial \mathbf{r}_t}{\partial u} \times \frac{\partial \mathbf{r}_t}{\partial \theta} = & \begin{vmatrix} \mathbf{i} & \mathbf{j} & \mathbf{k} \\ \mp \sin \alpha \cos \theta & \mp \sin \alpha \sin \theta & \cos \alpha \\ \left(R_t \mp \frac{\pi m}{4} \pm u \sin \alpha\right) \sin \theta & \left(R_t \mp \frac{\pi m}{4} \pm u \sin \alpha\right) \cos \theta & 0 \end{vmatrix} = \\ = & \left(R_t \mp \frac{\pi m}{4} \pm u \sin \alpha\right) (\cos \theta \cos \alpha \mathbf{i} + \sin \theta \cos \alpha \mathbf{j} \pm \sin \alpha \mathbf{k}), \end{aligned} \quad (3)$$

$$\mathbf{e}_t = \cos \theta \cos \alpha \mathbf{i} + \sin \theta \cos \alpha \mathbf{j} \pm \sin \alpha \mathbf{k}. \quad (2)$$

3.2. Double-edge milling cutter contact line equation

Let us assume the velocity of the workpiece and the tool to be \mathbf{v}_t and \mathbf{v}_g , respectively, at the engagement point,

with the relative speed being \mathbf{v}_{tg} . According to the engagement principle, the following engagement conditions should be met between the gear workpiece and the machining tool [16-19]:

$$\phi = \mathbf{n}_t \cdot \mathbf{v}_{tg} = \mathbf{n}_t \cdot \mathbf{v}_t - \mathbf{n}_t \cdot \mathbf{v}_g = 0. \quad (5)$$

Since $\mathbf{n}_t \cdot \mathbf{v}_t = 0$, Eq. (5) can be rewritten as

$$\phi = \mathbf{n}_t \cdot \mathbf{v}_g = \mathbf{e}_t \cdot \mathbf{v}_g = 0, \quad (6)$$

$$\mathbf{r}_g = \left[-\left(R_t \mp \frac{\pi}{4} m \pm u \sin \alpha \right) \cos \theta + R_g \psi + R \right] \mathbf{i} - \left(R_t \mp \frac{\pi}{4} m \pm u \sin \alpha \right) \sin \theta \mathbf{j} + (u \cos \alpha - R_g) \mathbf{k}, \quad (7)$$

$$\mathbf{v}_g = \omega_g \mathbf{k}_g \times \mathbf{r}_g - \omega_g R_g \mathbf{i} = \omega_g (\mathbf{k}_g \times \mathbf{r}_g - R_g \mathbf{i}), \quad (8)$$

$$\begin{aligned} \mathbf{e}_t \cdot \mathbf{v}_g &= -\omega_g u \cos^2 \alpha \cos \theta \pm \omega_g \sin \alpha \left[-\left(R_t \mp \frac{\pi}{4} m \pm u \sin \alpha \right) \cos \theta + R_g \psi + R_t \right] \\ &= -\omega_g \left[u \cos \theta \pm \sin \alpha \cos \theta \left(R_t \mp \frac{\pi}{4} m \right) \mp \sin \alpha (R_g \psi + R_t) \right] = 0. \end{aligned} \quad (9)$$

Then, the engagement conditions are:

$$u = \mp \frac{\sin \alpha \cos \theta \left(R_t \mp \frac{\pi}{4} m \right) - \sin \alpha (R_g \psi + R_t)}{\cos \theta}. \quad (10)$$

Therefore, the contact line equation between the tool and the gear workpiece becomes

$$\begin{cases} x_t = -\left(R_t \mp \frac{\pi}{4} m \pm u \sin \alpha \right) \cos \theta \\ y_t = -\left(R_t \mp \frac{\pi}{4} m \pm u \sin \alpha \right) \sin \theta \\ z_t = u \cos \alpha \\ u = \mp \frac{\sin \alpha \cos \theta \left(R_t \mp \frac{\pi}{4} m \right) - \sin \alpha (R_g \psi + R_t)}{\cos \theta} \end{cases}. \quad (11)$$

3.3. C-gear tooth surface equation

The expression for the contact line equation becomes the C-gear tooth surface equation in the $O_d - x_d, y_d$,

$$\mathbf{M}_{dt} = \mathbf{M}_{dg} \mathbf{M}_{gt} = \begin{bmatrix} \cos \psi & \sin \psi & 0 & R_g \psi \cos \psi \\ -\sin \psi & \cos \psi & 0 & -R_g \psi \sin \psi \\ 0 & 0 & 1 & 0 \\ 0 & 0 & 0 & 1 \end{bmatrix} \begin{bmatrix} 1 & 0 & 0 & R_t \\ 0 & 0 & 1 & -R_g \\ 0 & -1 & 0 & 0 \\ 0 & 0 & 0 & 1 \end{bmatrix} \quad (14)$$

and the tooth surface equation can be obtained as

$$\begin{bmatrix} x_d \\ y_d \\ z_d \\ 1 \end{bmatrix} = \mathbf{M}_{dt} \begin{bmatrix} x_t \\ y_t \\ z_t \\ 1 \end{bmatrix}, \quad (15)$$

which can be expanded as

z_d coordinates. The matrix for the transformation from (i) the $O_t - x_t, y_t, z_t$ to the $O_g - x_g, y_g, z_g$ coordinates can be expressed as

$$\mathbf{M}_{gt} = \begin{bmatrix} 1 & 0 & 0 & R_t \\ 0 & 0 & 1 & -R_g \\ 0 & -1 & 0 & 0 \\ 0 & 0 & 0 & 1 \end{bmatrix} \quad (12)$$

and (ii) the $O_g - x_g, y_g, z_g$ to the $O_d - x_d, y_d, z_d$ coordinate system can be expressed as

$$\mathbf{M}_{dg} = \begin{bmatrix} \cos \psi & \sin \psi & 0 & R_g \psi \cos \psi \\ -\sin \psi & \cos \psi & 0 & -R_g \psi \sin \psi \\ 0 & 0 & 1 & 0 \\ 0 & 0 & 0 & 1 \end{bmatrix}. \quad (13)$$

Therefore, using Eqs. (12) and (13), the matrix for the transformation from the $O_t - x_t, y_t, z_t$ to the $O_d - x_d, y_d, z_d$ coordinate system becomes

$$\begin{cases} x_d = \left[-\left(R_t \mp \frac{\pi}{4} m \pm u \sin \alpha \right) \cos \theta + R_t + R_1 \psi \right] \cos \psi + (u \cos \alpha - R_g) \sin \psi \\ y_d = \left[\left(R_t \mp \frac{\pi}{4} m \pm u \sin \alpha \right) \cos \theta - R_t - R_g \psi \right] \sin \psi + (u \cos \alpha - R_g) \cos \psi \\ z_d = \left(R_t \mp \frac{\pi}{4} m \pm u \sin \alpha \right) \sin \theta \\ u = \mp \sin \alpha \frac{\cos \theta \left(R_t \mp \frac{\pi}{4} m \right) - (R_g \psi + R_t)}{\cos \theta} \end{cases} \quad (16)$$

4. C-gear modeling method

The steps for modelling the C-gear using MATLAB are shown in (Fig. 3).

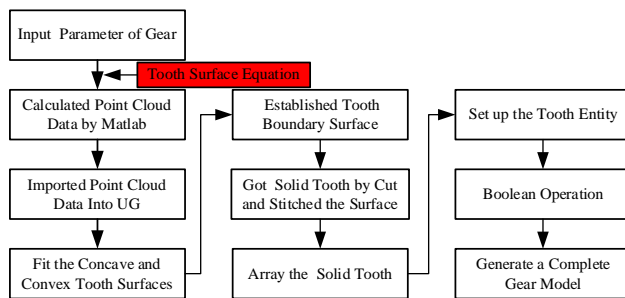


Fig. 3 Step-wise C-gear modelling method

The tooth surface parameters (ψ, θ) were uniformly dispersed, and the high-precision point cloud data of the tooth surface was calculated using Eq. (16). The point cloud data was subsequently imported into UG, and the "pass point" command was used to fit the high-precision concave

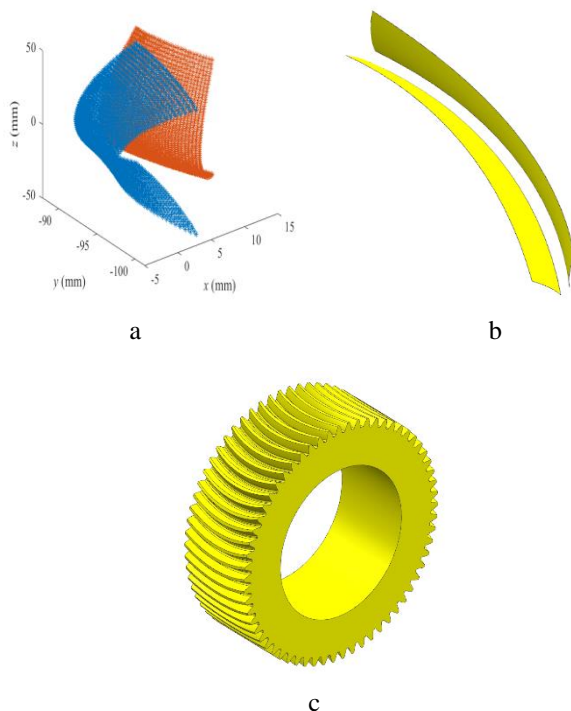


Fig. 4 Simplified process of high precision gear modelling: a – high-precision tooth point cloud data, b – fitting of the concave and convex tooth surfaces, c – completed gear model

and convex tooth surfaces. The high-precision gear model was then obtained by stitching and arraying (Fig. 4).

5. CNC machining technique

The workpiece material used for constructing the C-gear was No. 45 steel. The specific CNC machining process is shown in Fig. 5. The 45 steel gear blank with a thickness of 72 mm was first cut out using a sawing machine and roughed to the remaining 1 mm processing allowance on an ordinary lathe. Then the plane cutter of a 3-axis vertical CNC milling machine was used to reduce the height of the gear blank to 70 mm through double-sided milling (processing 1 mm per side). The round cake was also milled to correspond to the size of the outer circle. After machining the end face and the shape, the milling machine was used to construct the positioning hole of the gear. Subsequently, a 5-axis CNC machining center was used to complete the machining of the gear wheel.

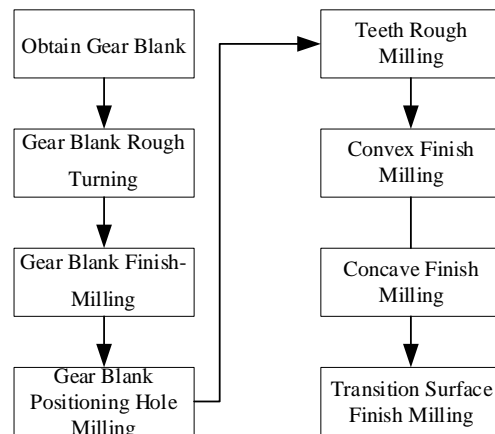


Fig. 5 CNC machining process for the C-gear

6. C-gear CNC machining process simulation

A driven gear with 62 teeth, a modulus of 5 mm, a tooth width of 40 mm, a pressure angle of 22.5° , a cutter radius of 300 mm, and a tool radius of 325 mm was studied. The simulation of the gear machining process was investigated using MASTERCAM.

6.1. Machining simulations

The C-gear processing flow using a 5-axis CNC machining center included setting the generated gear blank and milling its end faces and the outer diameter, machining of the gear blank positioning hole, rough machining of the teeth grooves and constructing their convex, concave, and

transition surfaces, gear machining simulation, and generating the CNC machining program. The 5-axis CNC machining center is shown in Fig. 6, the initial installation relationship between the tool and the workpiece is also shown in Fig. 6, and the overall tool path and processing results are shown in Fig. 7.

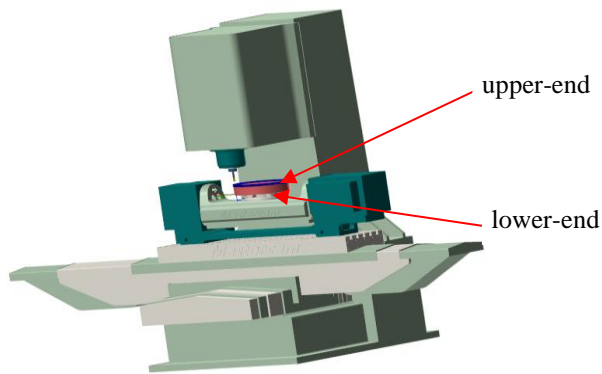


Fig. 6. 5-axis vertical CNC machining center

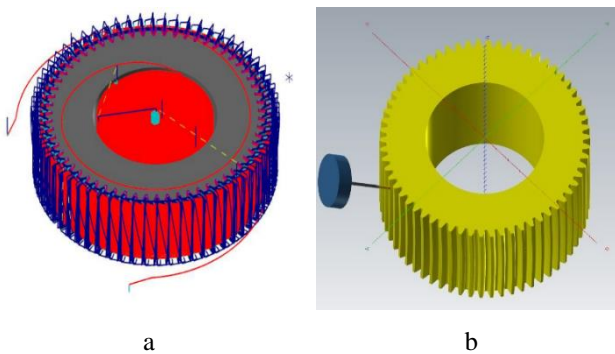


Fig. 7 Overall cutting tool path and processing results: a – overall cutting tool path, b – processing results

The specific steps for the tool path design and machining simulation using MASTERCAM are as follows:

Step 1. Setting up the generated gear blank: To ensure that the gear outer diameter and tooth width are 320 mm and 70 mm, respectively, the diameter and height of the generated gear blank were set to 322 mm and 72 mm, respectively, as the machining allowance of the outer profile and the end face was 2 mm.

Step 2. Milling of the gear blank end face: The two ends of the gear blank were finely machined using the plane milling cutter of a 5-axis vertical CNC milling machine. The height of the gear blank was milled to be 70 mm (double-sided milling with 1 mm being processed on each side). The tool path for the end face milling and contour machining are shown in Fig. 8. The upper and lower end faces were milled clockwise using a $\varnothing 80$ milling cutter under the following conditions: milling feed speed = 600, spindle speed = 1300, tool path = "plane milling", and machining volume = 1 mm (for each end face). The contour machining was implemented clockwise using a $\varnothing 12$ milling cutter under the following conditions: milling feed speed = 1500, spindle speed: 3500, tool path = "contour milling", and machining volume = 1 mm. Besides, tip correction is conducted, and the machining depth is 70 mm, with a depth of 2 mm each time.

Step 3. Machining of gear blank positioning hole: The 5-axis vertical CNC milling machine was used for

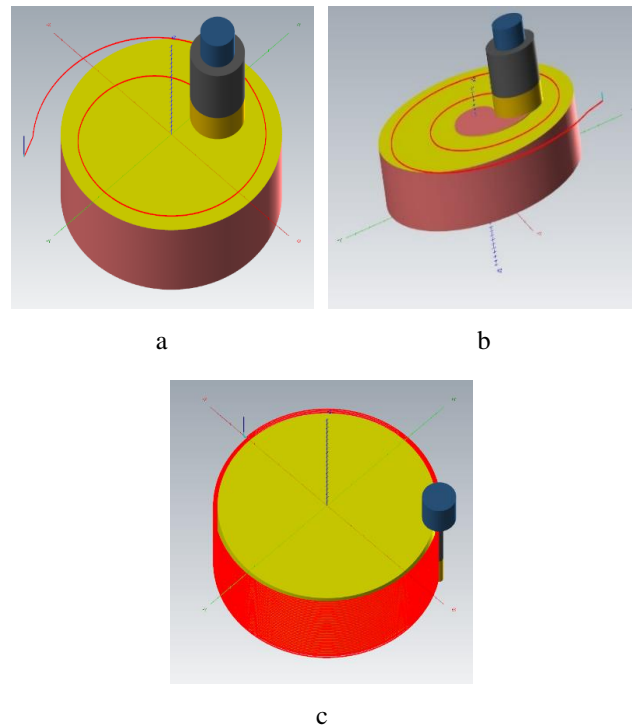


Fig. 8 Design schemes for the milling tool path: a – upper-end face, b – lower-end face, c – contour

the machining of the gear positioning hole with a diameter of 180 mm. Firstly, rough milling (axial-layered milling in a clockwise direction) and holing were performed using a $\varnothing 12$ milling cutter under the following conditions: milling feed speed = 1500, spindle speed = 3500, tool path = "2D high-speed tool path - dynamic milling", and machining depth = 70 mm. A finish machining allowance of 0.2 mm was reserved. Then, the machining was completed by milling in a clockwise direction using the $\varnothing 12$ milling cutter with tool path = "profile milling". The tool path of the gear blank positioning hole machining is shown in Fig. 9. In the Fig. 9, a expressed the rough milling tool path design schemes and Fig. 9, b expressed finish milling tool path design schemes for the gear blank positioning hole; and Fig. 9, c stood the actual rough milling and Fig. 9, d stood the finish milling tool paths for the gear blank positioning hole. At the same time, Fig. 9, c and Fig. 9, d further illustrate the starting and ending points of the tool, the tool position represents the end point of the tool path.

Step 4. Rough machining of a single gear tooth: Rough machining of a single gear tooth was completed using a $\varnothing 4$ milling cutter on the 5-axis vertical CNC milling machine under the following conditions: milling feed speed = 600, spindle speed = 5000, tool path = "advanced rotation" (clockwise), and finish machining allowance = 0.1 mm. Fig. 10 shows the tool path and machining results for the same.

Step 5. Rough machining of the overall gear teeth: After designing the tool path for a single gear tooth, this paper employed the rotating tool path function of MASTERCAM to construct all the teeth. The number of rotations was set to 62 to construct 62 equidistant gear teeth. The rest of the parameter values were the same as those mentioned in step 4. The tool path and rough machining results for the complete set of 62 gear teeth are shown in Fig. 11.

Step 6. Finish machining of gear tooth surfaces: After the rough machining of the gear blank mentioned in

steps 4 and 5, the gear teeth were essentially shaped as shown in Fig. 10, c. However, the surfaces of the gear teeth still show traces of tool cutting due to the feed volume, suggesting the requirement of finish machining of the concave,

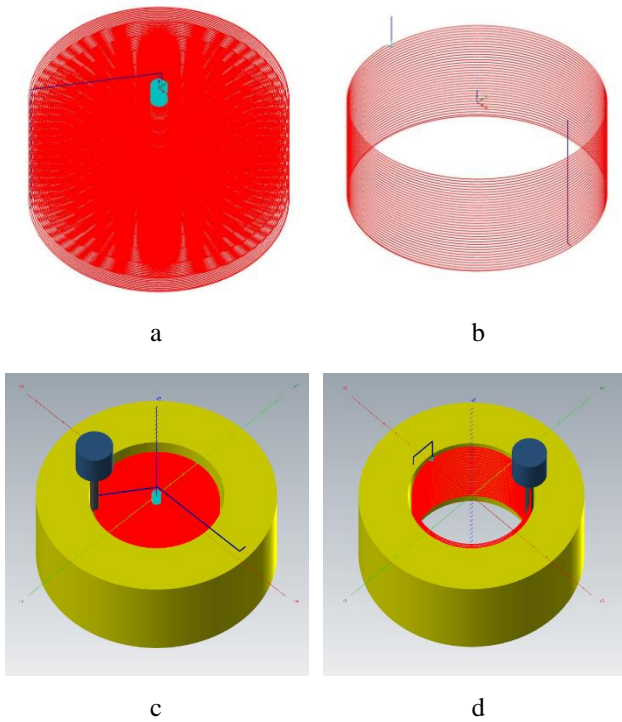


Fig. 9 Tool path of the gear blank positioning hole machining: a – rough milling, b – finish milling tool path design schemes for the gear blank positioning hole, c – rough milling, d – finish milling tool paths for the gear blank positioning hole

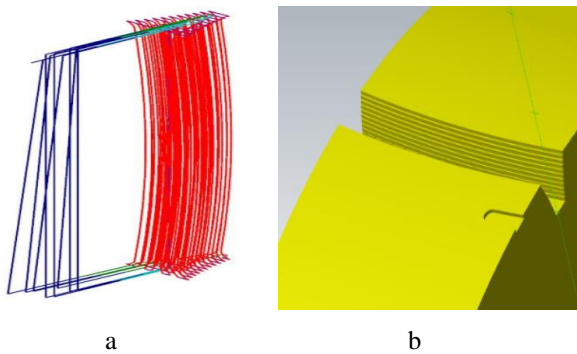


Fig. 10 Roughing tool path for a single gear tooth, a – tool path design, b – actual tool path

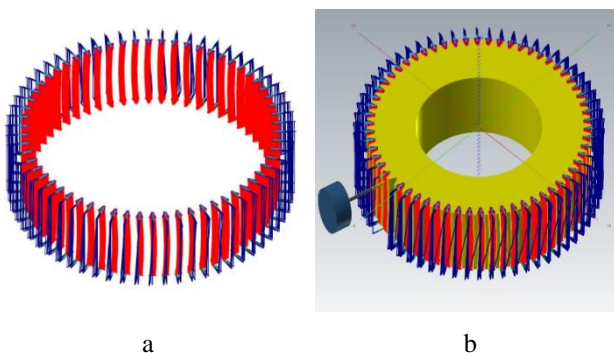


Fig. 11 Tool path and rough machining results for the complete set: a – tool path design, b – processing

convex, and transitional surfaces of the gears; tool paths were designed and implemented for this purpose (Figs. 12, 13 and 14). Fig. 12, a – Fig. 12, c respectively show the tool paths for the finishing of the three components of the gear groove. Fig. 12, a represents the machining tool path of the concave, Fig. 12, b represents the machining tool path of the convex, and Fig. 12, c represents the machining tool path of the transitional surfaces. Fig. 13, a – Fig. 13, c respectively shows the actual cutting path of the finishing tool for the three component surfaces of the gear groove, and also

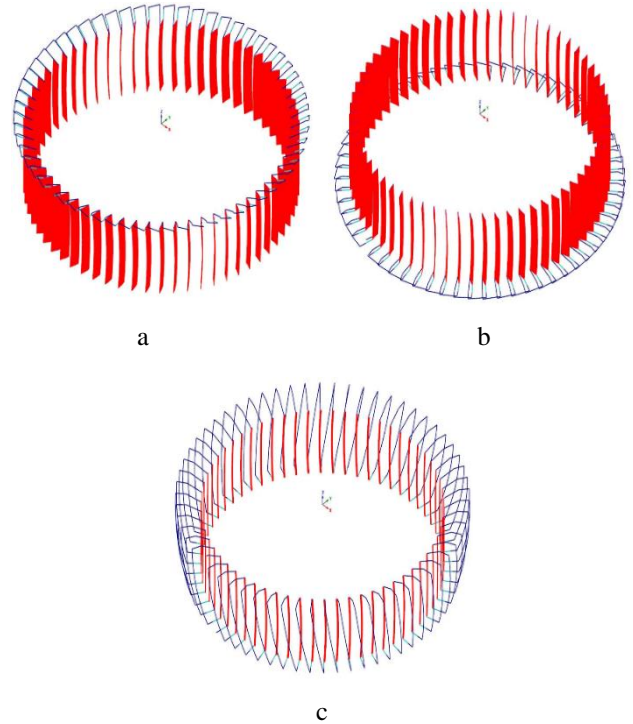


Fig. 12 Tool path designs for the finish machining: a – convex, b – concave, c – transitional gear tooth surfaces

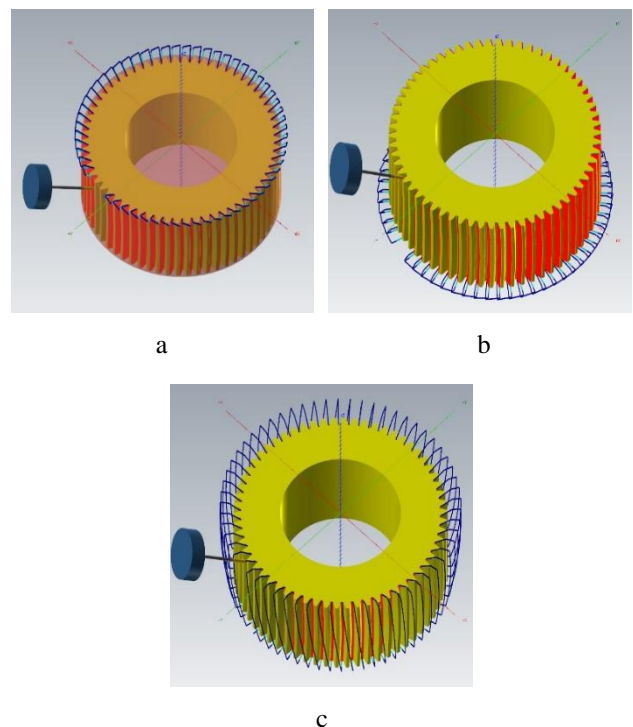


Fig. 13 Actual tool paths for the finish machining: a – convex, b – concave, c – transitional gear tooth surfaces

reflects the starting point and end point of the tool during the processing of the three component surfaces. Fig. 14, a – Fig. 14, c respectively shows the machining accuracy of the three components of the gear groove after finishing. Fig. 14, a represents the machining accuracy of concave, Fig. 14, b represents the machining accuracy of convex, and Fig. 14, c represents the machining accuracy of transitional surfaces. The finish machining of the gear teeth surfaces was carried out using a ball/round-nose milling cutter under the following conditions: milling feed speed = 600, spindle speed = 6000, and tool path = “intelligent synthesis”. The finish machining resulted in highly shiny convex, concave, and transitional gear teeth surfaces.

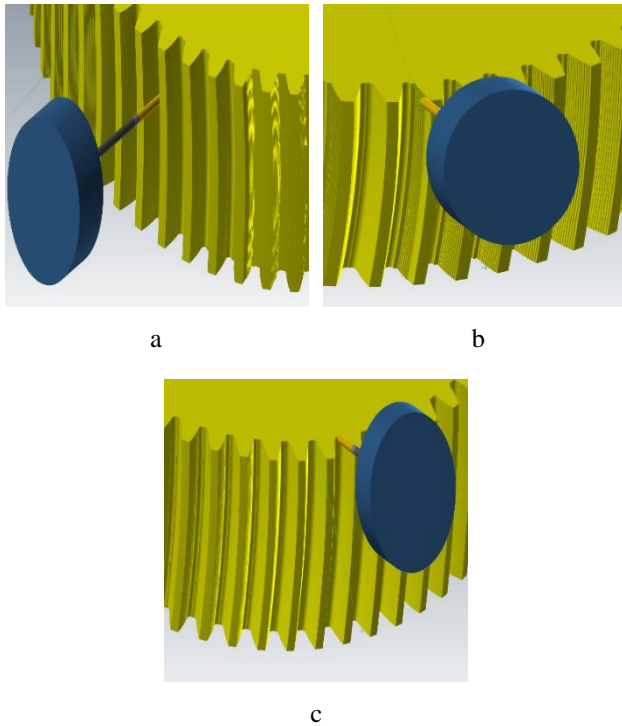


Fig. 14 Finish machining results: a – convex, b – concave, c – transitional gear tooth surfaces

6.2. Machining accuracy verification

As mentioned in the previous sections, the gear machining tool paths and simulation models were established using the MASTERCAM and VERICUT software. This paper further conducted comparative analyses of overcuts and residuals between the machined model and the original 3D model. The tolerance of overcuts and residuals was set to 0.01 mm for the real gear, and the corresponding distributions were obtained (Fig. 15). From the simulation results, 772 overcuts and 5000 residuals were found, with a maximum tolerance of 0.01 mm.

As this novel C-gear has a complex curved tooth surface, its machining accuracy has an important impact on the gear transmission performance. The surface overcut and residual tolerance values were set as shown in Fig. 16 and the actual overcuts and residuals on the machined gear tooth surfaces are shown in Fig. 17.

From the distribution of overcuts and residuals on the actual machined curved gear tooth surface, 1,823 overcuts were founded, with a maximum overcut of 0.094 mm, and 3,177 residuals, with a maximum residue of 0.094 mm,

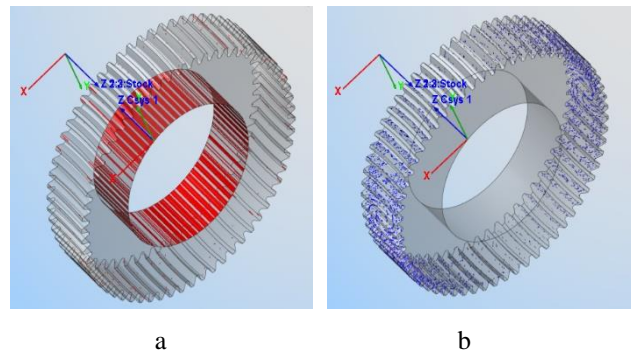


Fig. 15 Tolerance of overcuts and residuals from the simulation of gear machining: a – overcut, b – residual error distribution obtained

过切		残留	
范围 (毫米)	颜色	范围 (毫米)	颜色
0.10000	12:Thistle	0.10000	12:Thistle
0.06000	1:Red	0.06000	17:Magenta
0.05000	55:AutoDiff_G5	0.05000	60:AutoDiff_E5
0.04000	54:AutoDiff_G4	0.04000	59:AutoDiff_E4
0.03000	53:AutoDiff_G3	0.03000	58:AutoDiff_E3
0.02000	52:AutoDiff_G2	0.02000	57:AutoDiff_E2
0.01000	51:AutoDiff_G1	0.01000	56:AutoDiff_E1
0.00000	7:Light Sea Gr...	0.00000	7:Light Sea Gr...

Fig. 16 Surface overcut and residual tolerance value: a – overcut tolerance, b – residual tolerance

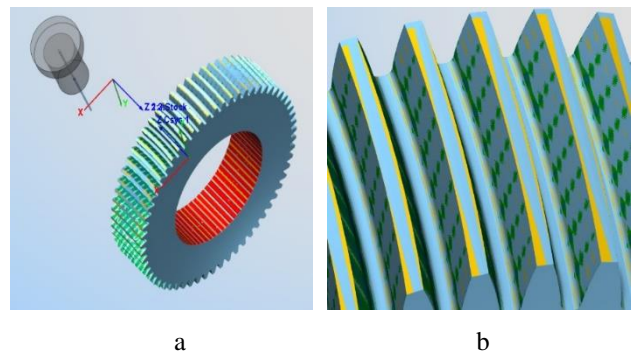


Fig. 17 Overcuts and residuals on the machined gear tooth surfaces: a – overcut, b – residual distribution

on the machining surface of the positioning holes. The maximum overcut volume was 0.02 mm on the tooth surface and 0.03 mm on the tooth root, and the maximum residual volume on both the tooth surface and root was 0.03 mm. In a previous study that employed a single-flute face milling disk cutter and a 6-axis CNC gear milling machine to construct a C-gear, the overcuts and residuals of the curved surface were found to be as follows [15]:

- 0.1 mm and < 0.06 mm of material residuals on the tooth root and surface, respectively, of the convex face;
- 0.06 mm and 0.04 mm of overcuts on the tooth root and tooth surface, respectively, and 0.06 mm of material residuals on the tooth surface of the concave face. Comprehensively comparing the maximum material residual and overcut results of [15], it can observe a vast improvement in

the error rates of our results. Moreover, as the actual machined tooth surface may exhibit a smaller machining error compared to the theoretical tooth surface, for the overcut and residual volumes, which included the error generated from the surface fitting during the 3D modelling of the gears. Therefore, this paper speculates a higher C-gear machining accuracy for the proposed method, with practically feasible tool paths and machining parameters.

7. Experimental analysis

The gear machining was completed using MASTERCAM according to the above-discussed machining steps and tool path simulations. After confirming the correct machining of each individual gear, the CNC code, which can be recognized by the machining center, was automatically generated using MASTERCAM and input into the TEMA DU650 5-axis CNC machining center (Fig. 18) to realize the construction of the novel high-speed, heavy-duty C-gears (Fig. 19).



Fig. 18 TEMA DU650 5-axis linkage CNC machining center

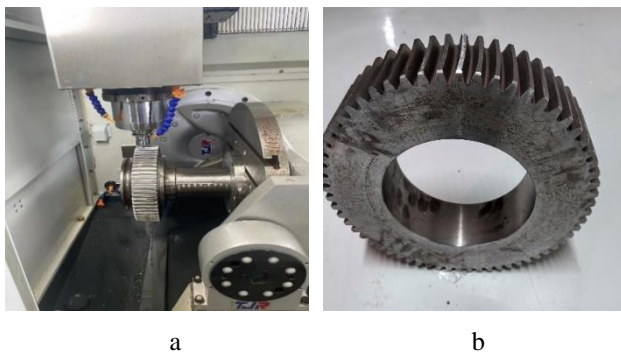


Fig. 19 Machining process and sample of new C gear: a – machining of gear teeth, b – finished C-gear

Fig. 19, a – Fig. 19, b show the machining process and finished gear of the new type C gear using TEMA DU650 5-axis CNC machining center. It can be seen from Fig. 19, a – Fig. 19, b that the NC machining process of the new type C gear designed in this paper can realize the NC machining of the new type C gear. At the same time, it can be seen from Fig. 19, b that the tooth surface of the new type C gear machined by the NC machining process designed in this paper has higher precision.

8. Conclusions

The construction of a C-gear and its improved models using specialized machines and rotary-tool milling machining methods may result in different products due to

the differences in the models, tool radii, and contour types of the machined objects. As a result, cutters and machining tools are of complexity, and it needs to design specialized machining machines. However, this type of machining increases the economic and time costs of the designing and manufacturing processes, and is not suitable for the prototype manufacturing of C-gears at the experimental research stage. Therefore, in this study proposed the use of 5-axis CNC machining center and designed the machining process to construct various types of C-gears. The MASTERCAM and VERICUT software were used to establish the corresponding C-gear machining tool path designs and simulation models. Finally, the machining of C-gears was realized using a TEMA DU650 5-axis CNC machining center.

For the gear machined by the proposed method, the maximum overcut volume was 0.02 mm on the tooth surface and 0.03 mm on the tooth root, and the maximum residual volume was 0.03 mm on both the tooth root and surface. These parameters were significantly better than those achieved.

The overcut volume and residual volume in the simulation results included both machining errors and errors generated by surface fitting during the 3D modelling of the gears. Therefore, the actual machined tooth surface is speculated to have smaller machining errors compared to the theoretical values. This method can be used for the prototype manufacturing of C-gears and their improved models in the present experimental research stage.

Acknowledgements

This work was supported by the National Natural Science Foundation of China (Grant No. 51875370) and the Natural Science Foundation of Sichuan Province (Grant No. 2022NSFSC0454, No. 2022NSFSC1975). Also Supported by Sichuan Science and Technology Program (Grant No. 2023ZYD0139). The authors thank TopEdit (www.topeditsci.com) for its linguistic assistance during the preparation of this manuscript.

References

1. **Arafa, H. A.** 2005. C-gears: geometry and machining, Proceedings of the Institution of Mechanical Engineers, Part C: Journal of Mechanical Engineering Science 219(7): 709–726. <http://dx.doi.org/10.1243/095440605X31481>.
2. **Ishibashi, A.** 1965. The characteristics of circular-arc-toothed cylindrical gears, Transactions of the Japan Society of Mechanical Engineers 31(225): 864–871. <http://dx.doi.org/10.1299/kikai1938.31.864>.
3. **Inoue, K.; Uematsu, S.** 1970. Method of roll forming on circular-arc gears, Journal of the Japan Society of Precision Engineering 36(430): 725–730. <http://dx.doi.org/10.2493/jjspe1933.36.725>.
4. **Tamotsu, K.** 1975. Method for cutting paired gears having arcuate tooth traces, US Patent No US-3915060-A. U.S. Patent and Trademark Office.
5. **Peng, F.** 1978. Research on circular arc tooth trace cylindrical gear based on Yuanla-method, Journal of Jilin University of Technology 1: 14-40 (In Chinese).
6. **Tseng, R.; Tsay, C.** 2001. Mathematical model and undercutting of cylindrical gears with curvilinear shaped teeth, Mechanism and Machine Theory 36(11-12):

- 1189–1202.
[http://dx.doi.org/10.1016/S0094-114X\(01\)00049-0](http://dx.doi.org/10.1016/S0094-114X(01)00049-0).
7. **Andrei, L.; Andrei, G.; Epureanu, A.; Oancea, N.; Walton, D.** 2002. Numerical simulation and generation of curved face width gears, *International Journal of Machine Tools and Manufacture* 42(1): 1–6.
[http://dx.doi.org/10.1016/S0890-6955\(01\)00101-8](http://dx.doi.org/10.1016/S0890-6955(01)00101-8).
 8. **Ma, Z.; Gong, Y.; Wang, X.** 2004. A new generating method for the machining of a cylindrical gear with symmetric arcuate tooth trace, *Journal of Xi'an Jiaotong University* 16(1): 18-21, 34 (In Chinese).
<http://dx.doi.org/10.3969/j.issn.1671-8267.2004.01.004>.
 9. **Ma, Z.; Deng, C.** 2012. CNC machining method of whole modified surface of cylindrical gears with arcuate tooth trace, *Journal of Mechanical Engineering* 48(5): 165-171. (In Chinese).
 10. **Tseng, J.; Tsay, C.** 2005. Mathematical Model and Surface Deviation of Cylindrical Gears With Curvilinear Shaped Teeth Cut by a Hob Cutter, *ASME Journal of Mechanical Design* 127(5): 982-987.
<http://dx.doi.org/10.1115/1.1876437>.
 11. **Tseng, J.; Tsay, C.** 2005. Undercutting and Contact Characteristics of Cylindrical Gears With Curvilinear Shaped Teeth Generated by Hobbing, *ASME Journal of Mechanical Design* 128(3): 634-643.
<http://dx.doi.org/10.1115/1.2181605>.
 12. **Dai, Y.; Yukinori, A.; Jiang, D.** 2006. Hobbing mechanism of cylindrical gear with arcuate tooth traces and experimental investigation, *China Mechanical Engineering* 17(7): 706-709 (In Chinese).
<http://dx.doi.org/10.3321/j.issn:1004-132X.2006.07.012>.
 13. **Song, A.; Wu, W. W.; Gao, S.; Gao, W-J.** 2010. The ideal geometry parameters of arch cylindrical gear and its process method. *Shanghai Jiaotong Daxue Xuebao/Journal of Shanghai Jiaotong University* 44: 1735-1740 (In Chinese).
 14. **Uzun, M.; Inan, A.** 2015. Manufacturing the new type concave–convex profile involute gears modeled by CAD–CAM in CNC milling machines, *Journal of the Brazilian Society of Mechanical Sciences and Engineering* 37(1): 255-261.
<http://dx.doi.org/10.1007/s40430-014-0170-y>.
 15. **Zhang, X.; Xie, Y.; Wang, P.** 2022. Machining method and simulation of line-contact curvilinear cylindrical gears, *Machine Tool & Hydraulics* 5(16): 150-154 (In Chinese).
<http://dx.doi.org/10.3969/j.issn.1001-3881.2022.16.028>.
 16. **Wu, Y.; Luo, P.; Bai, Q.; Liang, S.; Fan, Q.; Hou, L.** 2023. Modelling and analyzing of loaded meshing characteristics of cylindrical gear transmission with curvilinear-shaped teeth, *Meccanica* 58(8): 1555-1580.
<https://doi.org/10.1007/s11012-023-01690-1>.
 17. **Liang, S.; Wu, Y.; Hou, L.; Dong, L.; Fan, Q.; Zhang, H.** 2023. Research on influence mechanism of geometric error sources on tooth surface error of VH-CATT gear special machine tool, *The International Journal of Advanced Manufacturing Technology* 128(11–12): 5529-5546.
<http://dx.doi.org/10.1007/s00170-023-12001-z>.
 18. **Zhang, Q.; Wen, G.; Chen, Z.; Zhou, Q.; Xiang, G.; Yang, G.; Zhang, X.** 2022. Sensitivity Analysis Contact Reliability of VH-CATT Cylindrical Gear and Its Reliability with Material Strength Degradation, *International Journal of Foundations of Computer Science* 33(06n07): 691-716.
<http://dx.doi.org/10.1142/S0129054122420102>.
 19. **Zhang, Q.; Wen, G.; Chen, Z.; Zhou, Q.; Xiang, G.; Yang, G.; Zhang, X.** 2022. Contact stress reliability analysis based on first order second moment for variable hyperbolic circular arc gear, *Advances in Mechanical Engineering* 14(7): 16878132221111210.
<http://dx.doi.org/10.1177/16878132221111210>.

Q. Zhang, Z. Chen, Y. Xia, D. He, G. Xiang, G. Wen, X. Zhang, Y. Xie, G. Yang

COMPUTER NUMERICAL CONTROL MACHINING SIMULATIONS AND EXPERIMENTAL ANALYSIS OF A NOVEL C-GEAR

S u m m a r y

C-gear is a novel gear transmission system, with no existing special machining and cutting tools to realize its construction. In this study, we employed a 5-axis computer numerical control (CNC) machining center to construct a C-gear, while solving the prototype manufacturing problem at the experimental research stage. We deduced the C-gear mathematical model and studied the three-dimensional (3D) modeling methods based on the analysis of its generation principle. The C-gear processing technique using the 5-axis CNC machining center and the tool path designs were established using the VERICUT and MASTERCAM software, and the C-gears were experimentally constructed. The maximum overcut and residual of the gear positioning hole surface were both found to be 0.094 mm. Moreover, the maximum overcut on the tooth surface and root were 0.02 and 0.03 mm, respectively, and the maximum residual on both the tooth surface and root was 0.03 mm. The machining overcuts and residual amounts of the proposed method were better than those of reference [14]. The existing overcut and residual errors included the errors generated by surface fitting during the 3D modeling of the gears. Therefore, the machining errors of the physically constructed tooth surface are expected to be smaller than the theoretical value, suggesting a high feasibility of the proposed method to realize the machining of C-gears.

Keywords: C-gear, generation principle, mathematical model, computer numerical control machining technology, machining process simulation.

Received November 5, 2023
 Accepted August 19, 2024

